ISBN: 978-3-95450-184-7 doi:10.18429/JACoW-IPAC2018-THPAF037

BUNCH COMPRESSION AND TURNAROUND LOOPS IN THE FCC-ee INJECTOR COMPLEX

T.K. Charles*[1], School of Physics, University of Melbourne, Parkville, VIC 3010, Australia
M.J. Boland[2], Department of Physics and Engineering Physics, University of Saskatchewan, 116 Science Place, Saskatoon S7N 5E2, Saskatchewan, Canada
K. Oide, KEK, Oho, Tsukuba, Ibaraki 305-0801, Japan
F. Zimmerman, European Organization for Nuclear Research (CERN), Geneva, Switzerland
[1] also at European Organization for Nuclear Research (CERN), Geneva, Switzerland
[2] also at Canadian Light Source, University of Saskatchewan, Saskatoon, Saskatchewan, Canada

Abstract

The Future Circular e+e- Collider (FCC-ee) requires two 180-degree turnaround loops to transport the positron beam from the damping ring to the lower energy section of the linac. In addition bunch compression is required to reduce the RMS bunch length from 5 mm to 0.5 mm, prior to injection into the linac. A dogleg bunch compressor comprised of two triple bend achromat (TBAs) can achieve this compression. Sextupole magnets are incorporated into the bunch compressor design for chromaticity correction as well as optimisation of the second-order longitudinal dispersion, T_{566}, and to linearize the longitudinal phase space distribution. In this paper we present the design of the transport line and the bunch compressor. Measures to limit emittance growth due to coherent synchrotron radiation (CSR) are also discussed, because despite the relatively long bunch length, the large degree of bending required introduces cause for consideration of CSR.

FCC-ee INJECTOR LAYOUT

The FCC-ee project proposes an electron-positron collider of 100 km in circumference with luminosities of the order of $10^{35}\text{cm}^{-2}\text{s}^{-1}$ to enable precision measurements of several fundamental elementary particles, such as the Z and W bosons, the Higgs boson and the top quark [1].

One possible layout of the injector complex preceding the collider rings is shown in Fig. 1. Further details regarding the injector layout options can be found in [2]. Two 180 degree loops are needed to direct the positron beam from the damping ring back to the low energy (1.54 GeV) section of the linac for further acceleration. Immediately following the second turnaround loop, before the beam is injected back into linac, is the location of the bunch compressor. The possibility of using one or both of these turnaround loops for bunch compression was investigated, however the impact of CSR-induced emittance growth was found to be unmanageable without the inclusion of CSR compensation schemes such as those described in Refs. [3–7]. Instead the required bunch compression is performed by dogleg bunch compressor which is described in a later section. By delaying the bunch compression, and leaving the bunch length to be longer in the turnaround loops, makes the bunch less susceptible to CSR effects.

Table 1: Beam Properties at Damping Ring Exit

Property	Symbol	Value	Units
Beam energy	E_0	1.54	GeV
Bunch charge	Q	4.80	nC
Bunch length, initial	$\sigma_{z,i}$	5.00	mm
Energy spread	$\frac{\sigma_E}{E_0}$	0.10	%
Horizontal emittance	ϵ_x	1.81	nm rad
Vertical emittance	ϵ_y	0.37	nm rad

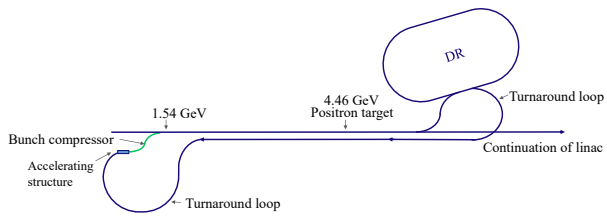

Figure 1: Section of the injector layout showing the position of the two turnaround loops. After passing through the Damping Ring (DR), the positrons are directed back to the 1.54 GeV section of the linac via the bunch compressor.

TURNAROUND LOOPS

The design of the turnaround loops needs to satisfy a number of criteria. The loops need to be globally isochronous and achromatic. The design must minimise transverse and longitudinal emittance growth. The footprint should be minimized to reduce tunnel cost. Table 1 summarizes the positron distribution properties coming from damping ring before injection into the turnaround loops.

The turnaround loop consists of Triple Bend Achromat (TBA) cells with 36.2 degrees of bending per cell. Figure 2 shows the magnet layout. The beam optics and dispersion functions for the 180 degree turnaround loop are shown in Fig. 3. The TBA layout limits the maximum R_{16} to ensure the transverse beam size does not grow too large (see Fig. 3b).

Particle tracking simulations were performed using `elegant` [8] to calculate the 1D model of CSR. The re-

* tessa.charles@cern.ch

ISBN: 978-3-95450-184-7 doi:10.18429/JACoW-IPAC2018-THPAF037

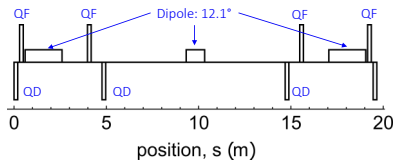

Figure 2: Magnet layout of the TBA cell of the turnaround loop.

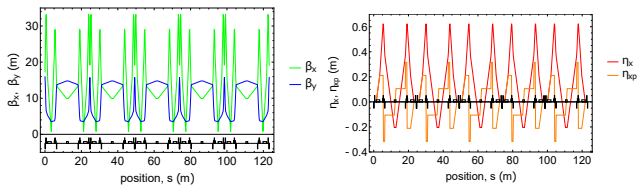

(a) (b)

Figure 3: (a) beta functions through the turnaround loop and (b) horizontal dispersion function.

sults show that through the turnaround loop, the increase in the horizontal emittance is limited to 2.5 %.

Figure 4 shows matrix element R_{56} returning to zero at the end of the cell. This illustrates that there is no momentum dependence on the total path length, i.e. the TBA is isochronous. Similarly the dispersion function returns to zero at the end of the TBA, indicating that the TBA is not only isochronous but also achromatic.

DOGLEG BUNCH COMPRESSOR

Before injection into the linac, the bunch length needs to be compressed from 5 mm to 0.5 mm. The relatively long initial bunch length places a limitation on the achievable linear energy-position correlation, or energy chirp, for a set energy spread. As a consequence, the R_{56} value required is reasonably large for a dogleg compressor. For an initial bunch length of 5 mm, and allowed rms energy spread of 1.1 %, the permissible energy chirp is $h_1 = \frac{1}{E_0}\frac{dE}{ds} = -2.19$ m^{-1}. As the aim is a final bunch length of 0.5 mm, the R_{56} value required is can be estimated using the following first-order approximation,

$$\frac{z_f}{z_i} = 1 + R_{56}h_1 \quad (1)$$

$$\sigma_{z,f} = |1 + R_{56}h_1|\sigma_{z,i} \quad (2)$$

where $\sigma_{z,i}$ and $\sigma_{z,f}$ are the initial and final rms bunch length respectively. Using Eq. (2), the R_{56} required is 0.41 m.

The energy chirp is imposed onto the beam by the S-band RF cavities upstream of the bunch compressor. The RF cavity has the properties of: $f_{RF} = 2.86$ GHz, $\phi_{RF} = 180°$, and an accelerating gradient of 22.3 MV/m. To achieve this R_{56} value, a dogleg compressor comprised of two TBAs was chosen. The TBAs are capable of achieving the reasonably large value of R_{56} due to the middle dipole, which creates bending in a non-zero dispersive region (see Fig. 5b). Note,

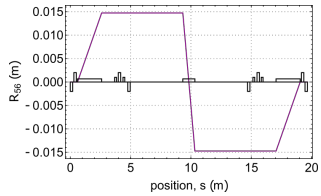

Figure 4: Longitudinal dispersion, R_{56} through one cell of turnaround loop.

here where we write relatively large, we refer to relatively large compared to other postive R_{56} dogleg compressors. A schematic of the bunch compressor layout is shown in Fig. 6. Each dipole has a bending angle of 11.25°, and between each dipole a quadrupole and a sextupole are placed to create a mirror symmetry across the achromat. Between the two TBAs is a section of adjusting the phase advance. The quadrupole magnets are used to control the dispersion function, ensuring it goes to zero at the end of each achromat.

The longitudinal dispersion properties of the bunch compressor are: $R_{56} = 0.40$ m, $T_{566} = 61.8$ mm, and $U_{5666} = -23.5$ mm, where T_{566} and U_{5666} are the second– and third-order longitudinal dispersion respectively. A benefit associated with the positive R_{56} compression, is that unlike a chicane, the bunch length gets progressively shorter towards the end of the compressor. Conversely, chicanes reach the shortest bunch length before the end of the compressor, before lengthening again by a small degree. This is sometimes refereed to as parasitic compression, due to the adverse effects the short bunch length can have with CSR production.

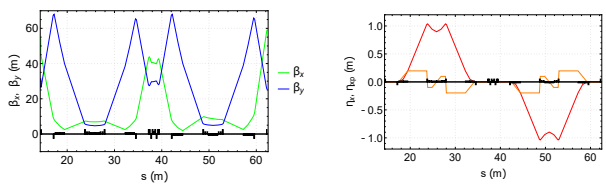

(a) (b)

Figure 5: (a) beta functions and (b) horizontal dispersion function through the dogleg bunch compressor.

Non-linear Terms

Unlike many bunch compression systems, the design presented here does not require a harmonic cavity [9–11]. Instead a form of optical linearization is used to minimise the non-linear terms encountered in bunch compression [12, 13]. Sextupole magnets are placed at a position where the dispersion is near maximum and are optimized for correcting the transverse chromaticity, rather than being optimized for cancellation of the second-order terms of the transport equations. Fortunately, despite being optimized for chromaticity, the resulting T_{566} is close to optimal for reducing the effect of the non-linear compression terms, negating the need for a harmonic cavity.

ISBN: 978-3-95450-184-7 doi:10.18429/JACoW-IPAC2018-THPAF037

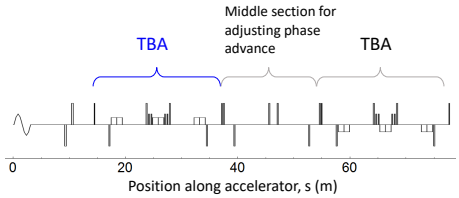

(a)

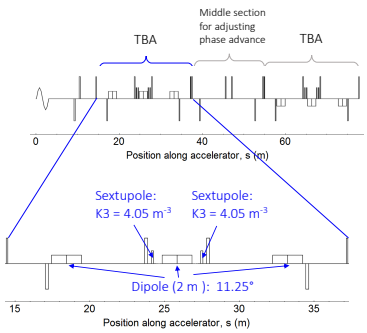

(b)

Figure 6: (a) Magnet layout of dogleg bunch compressor. The TBAs are identical except that they bend in opposite directions. (b) detailed layout of one TBA.

Figure 7 shows the final distribution both with and without the inclusion of sextupoles, where the initial uncorrelated energy spread has been artificially reduced to 0.01% so that the phase space distribution curvature is more clearly visible. It is clear from Fig. 7b that the sextupoles remove the curvature associated with the second-order dynamics, without the need for a harmonic cavity. A third-order component remains visible in the final distribution in Fig. 7b.

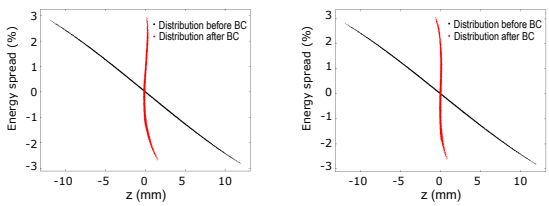

(a) (b)

Figure 7: Initial (black) and final (red) longitudinal phase space distributions for (a) without the inclusion of sextupoles and (b) with sextupoles included in bunch compressor. Note the initial uncorrelated energy spread was reduced to 0.01% for clarity of the non-linear effect.

INFLUENCE OF CSR

Left unchecked, CSR has the potential to significantly degrade the quality of the beam. This is true despite the relatively long bunch length ($\sigma_{z,f}$ = 0.5 mm) because the reasonably large R_{56} value required necessitates a large degree of bending. Fortunately, CSR cancellation techniques [3–7] can mitigate the emittance growth to less than 10 %.

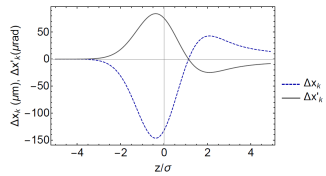

Figure 8: Typical CSR kicks in x and x' for one dipole.

Careful control of β_x and α_x in each dipole, as well as the phase advance between each dipole can allow us to cancel out the CSR kicks (Δx_k and $\Delta x'_k$) almost completely. Further work is being done to investigate the influence of non-typical CSR kicks. This can occur in dipoles 2 and 5 (i.e. the middle dipoles of each TBA) where the Twiss parameters are not constant along the length of the bunch, which can alter the shape of the CSR kick along the bunch. That is, the CSR kicks in dipoles 2 and 5 no longer follow the typical shape which is depicted in Fig. 8.

To compensate for the CSR kicks, an additional quadrupole magnet is needed in the section between the TBAs. A comparison of the emittance growth when this CSR kick analysis is applied and when it is not is shown in Fig. 9. Initially (i.e. before the CSR kick cancellation method applied), the horizontal emittance growth was 85.8 %. After the inclusion of the additional quadrupole, and the phase advance and Twiss parameters of the second TBA manipulated, the emittance growth was reduced to 6.8 % (which includes CSR in the drifts).

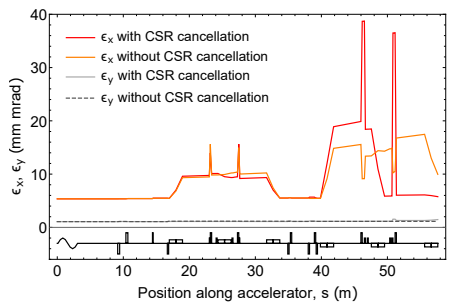

Figure 9: Emittance along the bunch compressor, before CSR cancellation technique applies (orange) and after (red).

CONCLUSION

A turnaround loop and bunch compressor were presented for the FCC-ee injector complex. Notably, the bunch compressor was a dogleg compressor comprised of two TBAs, for a positive R_{56}, and favourable T_{566}. CSR cancellation techniques were applied to minimise the emittance growth across the compressor to 6.8 %.

ACKNOWLEDGEMENT

T.K. Charles would like to acknowledge that this work was supported by the Victoria Fellowship. T.K. Charles also acknowledges S. Ogur for providing the details of the bunch exiting the FCCee damping ring.

ISBN: 978-3-95450-184-7 doi:10.18429/JACoW-IPAC2018-THPAF037

REFERENCES

[1] K. Oide, et al. "Design of beam optics for the future circular collider e+e- collider rings," *Phys. Rev. ST AB*, vol. 19, p. 111005, 2016.

[2] S. Ogur, et al. "Layout and Performance of the FCC-ee Pre-Injector Chain," presented at the 9th Int. Particle Accelerator Conf. (IPAC'18), Vancouver, Canada, Apr.-May 2018, paper MOPMF034, this conference.

[3] D. Douglas, "Suppression and Enhancement of CSR-Driven Emittance Degradation in the IR-FEL Driver," *Technical Report JLAB-TN-98-012*, 1998.

[4] S. Di Mitri, M. Cornacchia, and S. Spampinati, "Cancellation of coherent synchrotron radiation kicks with optics balance," *Phys. Rev. Lett.*, vol. 110, p, 014801, 2013.

[5] S. Di Mitri and M. Cornacchia, "Electron beam brightness in linac drivers for free-electron-lasers," *Phys. Rep.*, vol. 539, 2014.

[6] R. Hajima, "A first-order matrix approach to the analysis of electron beam emittance growth caused by coherent synchrotron radiation," *Japanese Journal of Applied Physics, Part 2: Letters*, vol. 42, pp. 974–976, 2003.

[7] Y. Jiao, X. Cui, X. Huang, and G. Xu, "Generic conditions for suppressing the coherent synchrotron radiation induced emittance growth in a two-dipole achromat," *Phys. Rev. ST AB*, vol. 17, p. 060701, 2014.

[8] M. Borland, "Elegant: A flexible SDDS-compliant code for accelerator simulation," Advanced Photon Source Report, LS-287, 2000.

[9] P. Emma, "X-Band RF Harmonic Compensation for Linear Bunch Compression in the LCLS," SLAC-TN-05-004, LCLS-TN-01-1, 2001.

[10] K. Flöttmann, T. Limberg, and P. Piot, "Generation of Ultra-short Electron Bunches by cancellation of nonlinear distortions in the longitudinal phase space," TESLA-FEL-2001-06, 2001.

[11] E. Vogal, M. Dohlus, H. Edwards, E. Harms, M. Huening, and K. Jensch, "Considerations on the third harmonic RF of the European XFEL," in *Proc. SRF'07*, Peking Univ., Beijing, China, paper WEP17, pp. 481–485, 2007.

[12] S. Thorin, M. Eriksson, S. Werin, D. Angal-Kalinin, J. McKenzie, B. Militsyn, and P. Williams, "Bunch Compression by Linearising Achromats for the MAX IV Injector," in *Proc. FEL'10*, Malmö, Sweden, paper WEPB34, pp. 471–474, 2010.

[13] Y. Sun, P. Emma, T. Raubenheimer, and J. Wu, "X-band RF driven free electron laser driver with optics linearization," *Phys. Rev. ST AB*, vol. 17, p. 110703, Nov 2014.